Applied Physics Letters

Atomic scale switches based on self-assembled surface magic clusters

Cite as: Appl. Phys. Lett. **112**, 253103 (2018); https://doi.org/10.1063/1.5036946
Submitted: 19 April 2018 • Accepted: 04 June 2018 • Published Online: 19 June 2018

Martin Franz, Chiara Panosetti, Jan Große, et al.

Atomic scale switches based on self-assembled surface magic clusters

Martin Franz,[1,a)] Chiara Panosetti,[2] Jan Große,[1] Tim Amrhein,[1] Karsten Reuter,[2] and Mario Dähne[1]
[1]*Institut für Festkörperphysik, Technische Universität Berlin, Hardenbergstr. 36, D-10623 Berlin, Germany*
[2]*Department Chemie, Technische Universität München, Lichtenbergstr. 4, D-85748 Garching, Germany*

(Received 19 April 2018; accepted 4 June 2018; published online 19 June 2018)

Atomic scale switches working at room temperature represent the ultimate level of device miniaturization. Using scanning tunneling microscopy, we find a bistable switching between two mirror-symmetric configurations of self-assembled magic rare earth silicide clusters on the Si(111) 7×7 surface. Density functional theory reveals an energy barrier of 1.3 eV between the two cluster configurations, suppressing the switching even at room temperature. However, intentional switching between the two states is possible in the presence of a close tunneling tip due to a tip-induced lowering of the energy barrier. *Published by AIP Publishing.* https://doi.org/10.1063/1.5036946

The miniaturization of electronic devices to achieve ever higher integration levels or storage densities is an ongoing challenge. The ultimate level of miniaturization is achieved for devices consisting of single atoms or molecules, which can be used as logic gates or memory cells. The first atomic scale switch consisting of atoms reversibly flipping between a surface and the tip of a scanning tunneling microscope (STM) was demonstrated already in 1991.[1] In the meantime, many other examples were realized, using STM to reversibly switch atoms or molecules between different states.[2–10] STM is the ideal technique for such experiments, as it combines atomic resolution imaging with the possibility of atomic manipulation.

However, most atomic scale switches realized so far only operate at cryogenic temperatures, since the small energy barrier between their different states can be easily overcome at room temperature, strongly hindering applications. The few reported atomic scale switches operating at room temperature are either constructed by atomic manipulation[10] being extremely slow or are based on randomly distributed molecules,[8,9] making large scale device fabrication difficult.

The Si(111) 7×7 surface[11] is an ideal template for the self-assembled growth of large quantities of very similar clusters. Here, identical, so-called magic clusters form within single 7×7 half unit cells after deposition of submonolayer amounts of different elements (e.g., Al, Ga, In, Pb, or Na) at moderate growth temperatures.[12–18] First, these clusters grow randomly distributed on the surface, while at higher coverages, perfectly ordered two-dimensional arrays can be fabricated.

Here, we report on the realization of atomic scale switches based on such self-assembled magic clusters on the Si(111) 7×7 surface operating at room temperature. Self-assembly allows the fabrication of an extremely large number of identical clusters within a very short period of time. Theoretically, cluster densities of up to 3.2×10^{13} cm^{-2} can be achieved on the Si(111) 7×7 surface.

The studied clusters are centered rare earth silicide clusters.[19,20] Using STM and density functional theory (DFT) calculations, we find that they form in two mirror symmetric configurations. Under appropriate tunneling conditions with the STM tip positioned close to the surface, the clusters show bistable switching between these configurations. This observation is explained by a rather large energy barrier of about 1.3 eV between the two cluster configurations suppressing a thermally excited switching even at room temperature. However, the barrier height is lowered in the presence of a closely approached STM tip leading to the switching. We also demonstrate reversible switching of the clusters.

All measurements were conducted at room temperature under ultra-high vacuum ($p \leq 10^{-8}$ Pa) using a home-built STM setup and electrochemically etched W tips. The detailed procedure for the preparation of the 7×7 reconstruction on the used *n*-type Si(111) samples is described elsewhere.[19,20] The rare earth metals Tb and Dy were deposited from W crucibles using electron beam evaporators. For cluster formation, the samples were heated during deposition. The deposition rate was calibrated using a quartz microbalance with an accuracy of $\pm 20\%$. All coverages are given in monolayers (MLs), with one monolayer (ML) corresponding to one rare earth atom per Si(111) surface unit cell (7.83×10^{14} atoms/cm^2).

All calculations were performed using density functional theory (DFT)[21,22] with the Perdew-Burke-Ernzerhof (PBE) semilocal exchange-correlation functional[23] as implemented in the FHI-aims package.[24] The latter relies on numeric atom-centered orbitals that are organized as different levels, or "tiers," of basis function groups of different angular momenta, as described in more detail by Blum *et al.* in Ref. 24. In the present calculations, the tight-tier II default basis set was employed. An initial geometry based on a best-guess match to the experimental STM images was locally optimized until the forces acting on each atom were smaller than 0.01 eV/Å. The supercell geometry setup contained a 6-layer Si(111) 7×7-reconstructed slab and 25 Å vacuum separation. The bottom layer was hydrogen passivated and the 3 bottom layers were kept frozen during relaxation. The Brillouin zone was sampled at the Γ-point. The transition path connecting the optimized geometry and its mirror image was optimized employing the climbing-image nudged elastic

a)Electronic mail: martin.franz@physik.tu-berlin.de

band (CI-NEB) method[25] with a chain of 5 images initialized as an image dependent pair potential (IDPP)[26] interpolation between the initial and final states, as implemented in the atomic simulation environment (ASE) python package.[27] STM simulations were performed within the Tersoff-Hamann model[28] and plotted at an isocurrent value of 10^{-6} e/Å^3.

The growth of rare earth silicide clusters on Si(111) 7×7 was already studied in our previous works.[19,20] At the used moderate growth temperatures, the structure of the 7×7 reconstruction essentially stays intact, acting as a template for the formation of the clusters. For both used rare earth metals, Tb and Dy, mainly two cluster types are observed forming either off-center or centered within the 7×7 half unit cells. Here, we concentrate on the centered clusters, which are predominantly observed for rare earth coverages between 0.04 ML and 0.1 ML and growth temperatures between 350 °C and 400 °C. An example of such a preparation is shown in Fig. 1(a) for Tb. A very similar growth behavior is found for Dy due to the chemical similarity of the trivalent rare earth metals, and thus is also expected for other trivalent rare earths. Under the used preparation conditions, mostly centered clusters form as indicated by blue triangles in Fig. 1(a). The clusters show a strong tendency for occupying the faulted half unit cells of the Si(111) 7×7 surface (indicated by F). Locally, the beginning formation of ordered arrays is already observed. However, due to an overlap of the growth regimes, different structures also appear occasionally, such as the bright features marked by black circles.

More detailed filled and empty state STM images of the centered Tb and Dy silicide clusters are shown in Figs. 1(b)–1(e). For both polarities, the clusters appear as triangles formed by three bright spots in the central region of the half unit cells, while the Si corner adatoms of the 7×7 reconstruction appear unchanged. However, while the clusters appear symmetrically with respect to the 7×7 half unit cell in the filled state images, they appear rotated by about 30° in the empty state images.

The appearance in the filled state images is very similar to the one of other centered cluster systems like the magic group-III metal clusters;[12–16] thus, we suggested a similar structure model in our previous publication on Dy silicide clusters based solely on filled state STM images.[19] However, the rotated appearance in the empty state images rules out such an atomic structure. Thus, an adapted structure model, developed on the basis of the present STM results as well as DFT calculations, was developed.

From the STM appearance of clusters as a triangle formed by three bright spots at both polarities, we deduce a RE_3Si_3 stoichiometry (RE stands for the respective rare earth). A DFT based structural optimization then results in the structure model shown in Figs. 2(a) and 2(b). This model nicely explains the experimental observations as demonstrated by the good agreement between the experimental [Figs. 1(b)–1(e)] and simulated STM images [Figs. 2(c) and 2(d)].

However, regarding the rare earth atoms, a second set of equivalent sites exists. Positioning the atoms at these sites

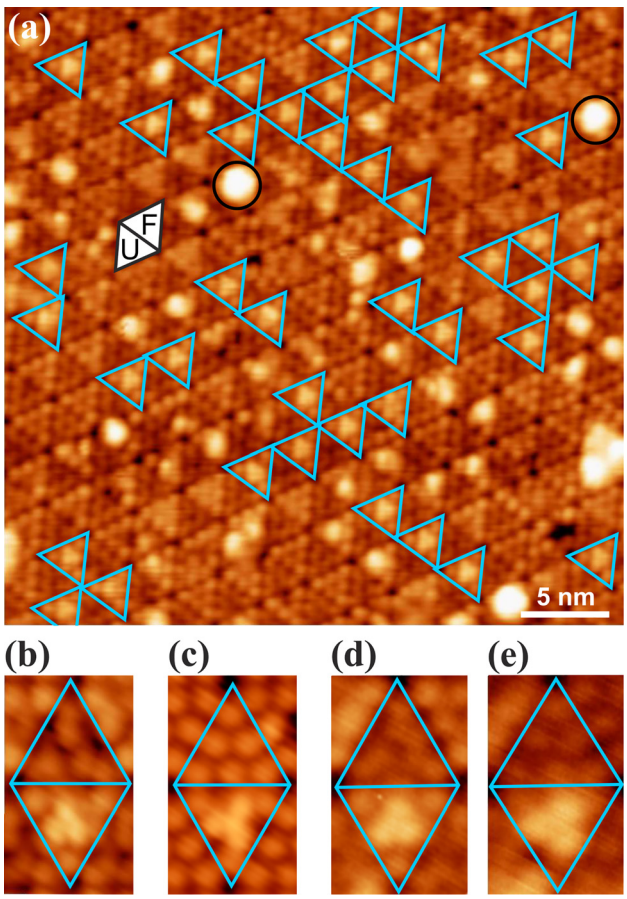

FIG. 1. Centered rare earth silicide clusters on Si(111) 7×7. (a) Overview filled state STM image of Tb silicide clusters grown by depositing 0.08 ML Tb at 360 °C (sample voltage $V_S = -2.0$ V; tunneling current $I_T = 100$ pA). The orientation of the faulted and unfaulted half unit cells of the Si(111) 7×7 reconstruction is indicated by F and U, respectively. Half unit cells with centered rare earth silicide clusters are marked by blue triangles, while occasionally observed bright features are marked by black circles. (b) Detailed filled state ($V_S = -2.0$ V; $I_T = 100$ pA) and (c) empty state ($V_S = +2.0$ V; $I_T = 100$ pA) images of centered Tb silicide clusters. (d) Detailed filled state ($V_S = -2.0$ V; $I_T = 100$ pA) and (e) empty state ($V_S = +2.0$ V; $I_T = 70$ pA) images of centered Dy silicide clusters.

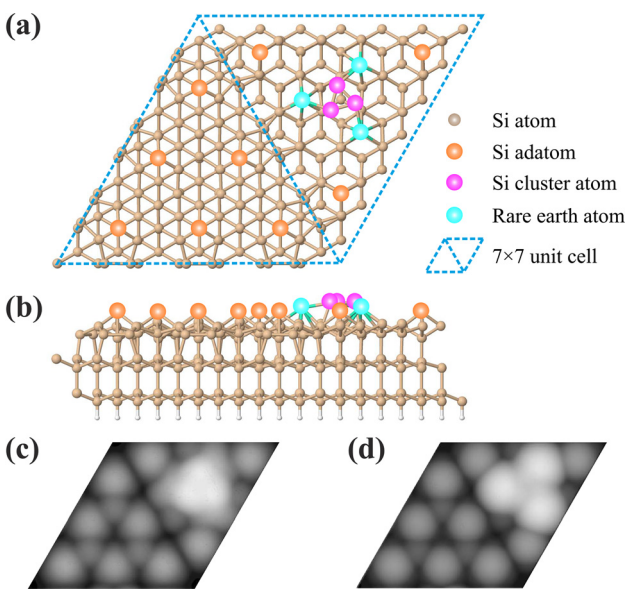

FIG. 2. Atomic structure of the centered rare earth silicide clusters. (a), (b) Structure model in (a) top view and (b) side view, as derived from DFT calculations. (c) Simulated filled state ($V_S = -2.0$ V) and (d) empty state ($V_S = +2.0$ V) STM images.

leads to a mirror symmetric cluster structure, which is indeed observed experimentally, as shown in Fig. 3. In the STM image shown in (a), two centered Tb silicide clusters are formed. The left one, indicated by a red triangle, appears rotated by 30° in the clockwise direction (denoted as right configuration), while the right one, indicted by a yellow triangle, shows a counterclockwise rotation (left configuration). In (b) and (c), the structure models for both configurations are shown. Both configurations have the same electronic structure, and they are observed with equal frequency, as also expected from their energetic equality.

Although the clusters can be imaged without change at room temperature even for hours, switching between the two configurations is observed under certain conditions, as shown in Fig. 4. In (a)–(d), a series of STM images acquired at different tunneling voltages is presented in the order they were recorded. All images show the same region of the surface with two centered Tb silicide clusters. At a relatively large negative sample bias, as shown in (a), the clusters appear symmetrically as described earlier, and their configurations are thus not distinguishable. Only with a positive polarity of the tunneling bias, as shown in (b), the configuration of the clusters becomes visible. In this case, both clusters are initially in the right configuration, as indicated by red triangles. However, at a lower positive tunneling bias, as shown in (c), the configuration of the cluster cannot be identified any more. Here, only a fuzzy signal appears at the locations of the clusters, indicating a motion of the clusters being too fast for STM imaging. Indeed, when increasing the tunneling bias again as shown in (d), the image of the clusters becomes stable again. Yet, in contrast to the image in (b), one cluster is now found in the left configuration as indicated by a yellow triangle. The fuzzy appearance at the low positive voltage can thus be assigned to a repetitive switching between the two configurations. After increasing the voltage again, the clusters then stabilize again.

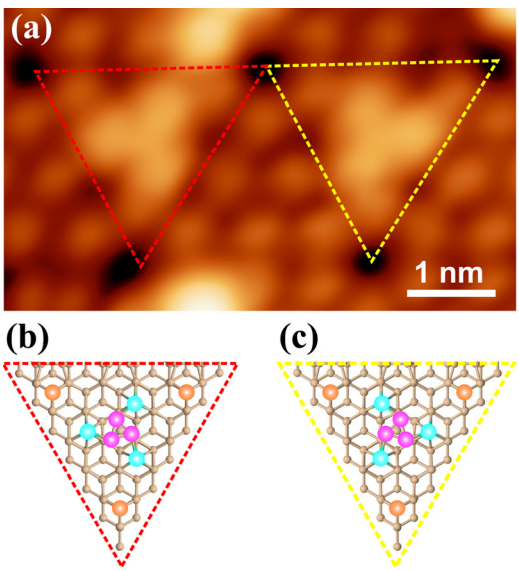

FIG. 3. The two configurations of the RE_3Si_3 clusters. (a) Empty state STM image of two centered Tb silicide clusters ($V_S = +1.5$ V; $I_T = 100$ pA), one in the right configuration (marked by the red triangle) and one in the left configuration (yellow triangle). In (b) and (c), the corresponding structure models are shown.

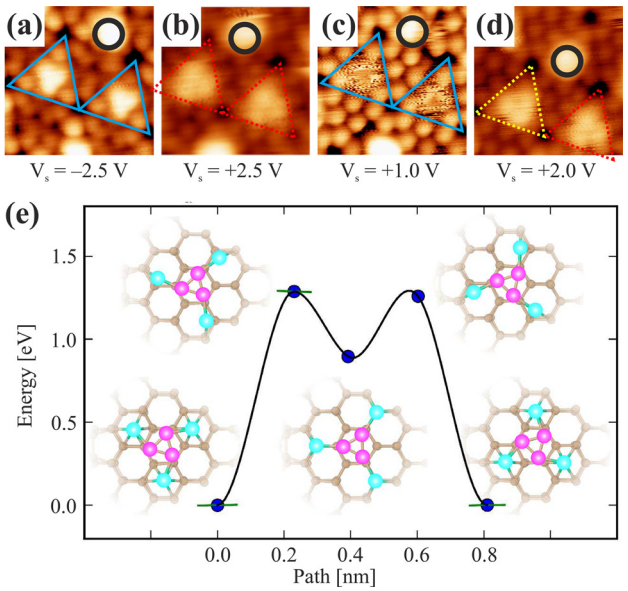

FIG. 4. Tip induced switching of the RE_3Si_3 clusters. (a)–(d) Series of STM images of the same surface area with two centered Tb silicide clusters, in the order they were recorded. The bright feature marked by a black circle is used as a spatial reference. All images were recorded with $I_T = 100$ pA, the tunneling bias is given below the images. (e) Energy barrier for the path from the right to the left configuration, calculated for centered Tb silicide clusters. The insets show the respective cluster structure at the points indicated in the curve.

In order to investigate this behavior in more detail, the energy barrier between the two cluster configurations was calculated using the CI-NEB method.[25] The result is shown in Fig. 4(e). The two configurations form equally deep minima, while the energy increases along the path between them. The barrier of about 1.3 eV is rather high, nicely explaining the suppression of thermally induced switching at room temperature. In the center of the path, a third relative minimum of the curve is found corresponding to a symmetric configuration of the RE_3Si_3 clusters. We do not observe this symmetric configuration experimentally, what we assign to the much smaller energy barrier of about 0.4 eV that can be overcome easily by thermal excitation at room temperature, leading to the relaxation of the clusters into either the left or the right configuration.

Since the switching occurs only under certain tunneling conditions, the presence of the STM tip must have a considerable influence on the barrier height. All images shown here were recorded in a constant current mode, with a feedback loop adjusting the tip height. In this mode, the tip sample distance is smaller for lower absolute tunneling voltages. At high tunneling voltages, as shown, e.g., in Figs. 4(b) and 4(d), the tip is rather far away from the surface and no switching occurs. Only at relatively low voltages and thus also smaller tip-sample distances, the clusters start to switch between the two configurations [Fig. 4(c)]. Hence, we can relate the onset of switching to an interaction with the approaching STM tip that is lowering the barrier height, which can then be overcome by thermal excitation. It should be noted that, using different tips, we sometimes observe the switching already at higher tunneling voltages or we do not observe any switching at tunneling conditions similar to those shown in Fig. 4(c). This is assigned to different atomic

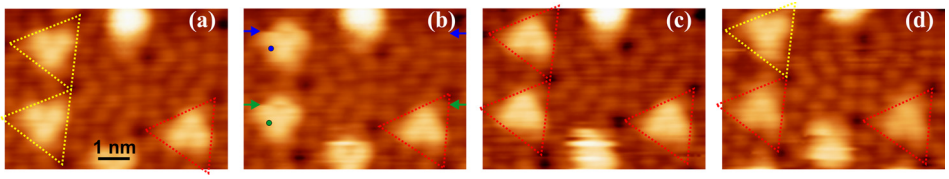

FIG. 5. Reversible switching of the RE_3Si_3 clusters. (a)–(d) STM images of three centered Tb silicide clusters ($V_S = +2.5$ V; $I_T = 100$ pA). Switching procedures were performed at the positions indicated by circles after scanning the lines indicated by equally colored arrows.

structures and/or terminations of the STM tips, which are expected to have a considerable influence on the tip-cluster interaction.

The lowering of the barrier height for the closely approached STM tip is now used to intentionally switch the clusters from one configuration to the other, as shown in Fig. 5. At first, the initial configuration of the clusters is determined by recording an image under stable imaging conditions as shown in (a). In the imaged area, there are three clusters. Initially, two clusters are found in the left configuration and one in the right configuration. During acquisition of (b), the two clusters on the left side of the image are switched from the left to the right configuration, as demonstrated by the image shown in (c) that was recorded directly after (b). For this purpose, after scanning the lines indicated by the arrows, the tip was placed above the respective cluster at the positions indicated by the equally colored circles. At these positions, the tip height was strongly reduced by 600 pm with the feedback loop turned off, leading to the lowering of the energy barrier and a thermally induced switching of the clusters. As the switching was performed when interrupting the scanning of the respective clusters, the final cluster configuration can already be seen in (b) in the region above the scan lines of the switching process (the scan is performed from bottom to top). This leads to the rectangular appearance of the clusters in (b), being a combination of images of the two configurations. Between images (c) and (d), the same procedure was again performed for the cluster in the upper left corner in order to switch it back to the left configuration. The back-switching is demonstrated by the STM image (d) showing the final configurations of the clusters. No switching procedures were performed on the cluster on the right side, which keeps its configuration during the whole image series. This demonstrates that the switching is really limited to the cluster underneath the closely approached STM tip.

In summary, we investigated centered rare earth silicide clusters using STM and DFT. The clusters with RE_3Si_3 stoichiometry form in two mirror symmetric configurations and show a bistable switching between these configurations at room temperature under certain tunneling conditions. This behavior is explained by a rather large energy barrier of about 1.3 eV separating the two configurations. In the presence of a closely approached STM tip, the barrier height is lowered and the clusters can switch between the configurations. We could even demonstrate the reversible switching of the clusters. It should be noted that, in the present experiments, the end configuration of the switching is random. However, placing the tip accurately above a certain part of a cluster should lead to an asymmetric energy barrier and might enable the switching of the clusters to a certain configuration. In this way, the combination of controlled switching at room temperature with self-assembled growth demonstrated here makes these clusters promising for future ultra-high density memory devices.

The authors thank the Deutsche Forschungsgemeinschaft for financial support through FOR 1282, projects D and H. C.P. and K.R. gratefully acknowledge the Gauss Centre for Supercomputing e.V. (www.gauss-centre.eu) for funding this project by providing computing time on the GCS Supercomputer SuperMUC at Leibniz Supercomputing Centre (www.lrz.de) under Grant No. PR92ME.

[1]D. Eigler, C. Lutz, and W. Rudge, Nature **352**, 600 (1991).
[2]U. Quaade, K. Stokbro, C. Thirstrup, and F. Grey, Surf. Sci. **415**, L1037 (1998).
[3]Y. Mo, Science **261**, 886 (1993).
[4]P. Liljeroth, J. Repp, and G. Meyer, Science **317**, 1203 (2007).
[5]C. Nacci, J. Lagoute, X. Liu, and S. Fölsch, Phys. Rev. B **77**, 121405 (2008).
[6]C. Nacci, S. Fölsch, K. Zenichowski, J. Dokić, T. Klamroth, and P. Saalfrank, Nano Lett. **9**, 2996 (2009).
[7]F. Mohn, J. Repp, L. Gross, G. Meyer, M. S. Dyer, and M. Persson, Phys. Rev. Lett. **105**, 266102 (2010).
[8]M. El Garah, B. Baris, V. Luzet, F. Palmino, and F. Chrioux, ChemPhysChem **11**, 2568 (2010).
[9]J. Liu, C. Li, X. Liu, Y. Lu, F. Xiang, X. Qiao, Y. Cai, Z. Wang, S. Liu, and L. Wang, ACS Nano **8**, 12734 (2014).
[10]E. Inami, I. Hamada, K. Ueda, M. Abe, S. Morita, and Y. Sugimoto, Nat. Commun. **6**, 6231 (2015).
[11]K. Takayanagi, Y. Tanishiro, M. Takahashi, and S. Takahashi, J. Vac. Sci. Technol., A **3**, 1502 (1985).
[12]M. Lai and Y. Wang, Phys. Rev. B **64**, 241404 (2001).
[13]J.-F. Jia, J.-Z. Wang, X. Liu, Q.-K. Xue, Z.-Q. Li, Y. Kawazoe, and S. Zhang, Appl. Phys. Lett. **80**, 3186 (2002).
[14]M. Franz, J. Schmermbeck, and M. Dähne, J. Vac. Sci. Technol., B **34**, 04J101 (2016).
[15]V. Kotlyar, A. Zotov, A. Saranin, T. Kasyanova, M. Cherevik, I. Pisarenko, and V. Lifshits, Phys. Rev. B **66**, 165401 (2002).
[16]J.-L. Li, J.-F. Jia, X.-J. Liang, X. Liu, J.-Z. Wang, Q.-K. Xue, Z.-Q. Li, J. Tse, Z. Zhang, and S. Zhang, Phys. Rev. Lett. **88**, 066101 (2002).
[17]S.-C. Li, J.-F. Jia, R.-F. Dou, Q.-K. Xue, I. Batyrev, and S. Zhang, Phys. Rev. Lett. **93**, 116103 (2004).
[18]K. Wu, Y. Fujikawa, T. Nagao, Y. Hasegawa, K. Nakayama, Q. Xue, E. Wang, T. Briere, V. Kumar, Y. Kawazoe, S. Zhang, and T. Sakurai, Phys. Rev. Lett. **91**, 126101 (2003).
[19]M. Franz, S. Appelfeller, M. Rychetsky, and M. Dähne, Surf. Sci. **609**, 215 (2013).
[20]M. Franz, J. Große, R. Kohlhaas, and M. Dähne, Surf. Sci. **637-638**, 149 (2015).
[21]P. Hohenberg and W. Kohn, Phys. Rev. **136**, B864 (1964).
[22]W. Kohn and L. J. Sham, Phys. Rev. **140**, A1133 (1965).
[23]J. P. Perdew, K. Burke, and M. Ernzerhof, Phys. Rev. Lett. **77**, 3865 (1996).
[24]V. Blum, R. Gehrke, F. Hanke, P. Havu, V. Havu, X. Ren, K. Reuter, and M. Scheffler, Comput. Phys. Commun. **180**, 2175 (2009).
[25]G. Henkelman, B. P. Uberuaga, and H. Jónsson, J. Chem. Phys. **113**, 9901 (2000).

[26]S. Smidstrup, A. Pedersen, K. Stokbro, and H. Jónsson, J. Chem. Phys. **140**, 214106 (2014).
[27]A. H. Larsen, J. J. Mortensen, J. Blomqvist, I. E. Castelli, R. Christensen, M. Duak, J. Friis, M. N. Groves, B. Hammer, C. Hargus, E. D. Hermes, P. C. Jennings, P. B. Jensen, J. Kermode, J. R. Kitchin, E. L. Kolsbjerg, J. Kubal, K. Kaasbjerg, S. Lysgaard, J. B. Maronsson, T. Maxson, T. Olsen, L. Pastewka, A. Peterson, C. Rostgaard, J. Schitz, O. Schtt, M. Strange, K. S. Thygesen, T. Vegge, L. Vilhelmsen, M. Walter, Z. Zeng, and K. W. Jacobsen, J. Phys.: Condens. Matter **29**, 273002 (2017).
[28]J. Tersoff and D. Hamann, Phys. Rev. Lett. **50**, 1998 (1983).